Paper:

Muscle Synergy Analysis Between Young and Elderly People in Standing-Up Motion

Qi An, Yusuke Ikemoto, and Hajime Asama

The University of Tokyo
7-3-1 Hongo, Bunkyou-ku, Tokyo 113-8656, Japan
E-mail: anqi@robot.t.u-tokyo.ac.jp
[Received May 13, 2013; accepted October 23, 2013]

Standing up is fundamental to daily activities of the elderly. It is necessary both to enhance muscle strength and to strengthen muscle coordination for improvement of their motor function. In this paper, we extract important data related to muscle coordination, called synergy, to perform standing motion by young and elderly participants. The contribution of muscle synergy to body kinematics is calculated through neural networks that estimate joint torque and body kinematics. To explain deficient motor function in elderly persons, extracted synergy is classified into 4 clusters based on how synergy contribute to body kinematics. Cluster analysis explains that elderly participants have weaker synergy than young persons in bending their backs to generate momentum. Compared to younger persons, older persons require additional muscle coordination to stabilize posture after standing-up in order to avoid falling.

Keywords: standing-up motion, muscle synergy, aging, neural networks

1. Introduction

The aging society has raised severe healthcare issues in developed countries. As life expectancy increases, the ratio of elderly to young individuals has increased rapidly, potentially decreasing the quality of life for both old and young persons. For the elderly, activities of daily living (ADL) – getting up from a bed or chair, dressing, or using the toilet – often become more difficult with age [1]. Similarly, informal family caregivers suffer physical and mental stress due to the unfamiliar tasks [2]. To improve this situation, preventive medicine has been suggested to enable the elderly to take more care of themselves. Many assistive systems, such as care beds or external exoskeletons, have been developed to enhance ADL for the elderly. Assistive robotics, in fact, can aid deficient body functions, but preventive medicine has not been widely implemented yet. In this study, we focus on standing up motion because the elderly who are not able to perform this basic action have difficulty in mobility necessary for ADL [3, 4]. Preventing individuals from becoming bedridden requires both supplementing their insufficient strength and retraining their motor control. There are many previous studies which focus on training methodology to train motor control of elderly persons. It is known that the elderly can enhance muscle strength [5], but training a single muscle may not improve functional ability. Motor function performance decreased only when muscle strength was below a certain threshold [6, 7]. It is therefore implied that as long as the elderly persons have a certain amount of muscle strength, training a single muscle would not improve motor function.

On the other hand, it has been reported that training should examine the activation of different kinds of muscles specifically to improve motor ability [8]. Complex human motion usually consists of moving different muscles and joints, so the effect of training a single muscle is limited. To enhance motor function – as opposed to muscle strength – it is important to know what groups of muscles are activated together to generate motion.

In this study, the synergy hypothesis is used to extract necessary groups of muscle activation from the standing. The idea was originally introduced by Bernstein, who suggested that complex human motion be divided into simplified modules of coordinated muscle activation called synergy [9]. Some recent studies have shown that complex human motor tasks are simplified by small sets of muscle coordination [10, 11]. If muscle coordination (synergy) differs between the elderly and younger persons, it would be useful to develop training methodology specifically for the deficient synergy of the elderly.

Our objectives in this paper are thus to extract synergies necessary to achieve standing-up from both the elderly and the young. Synergies are also classified into several groups based on its contribution to standing-up motion, and how muscle synergy differs between the elderly and the young is explained.

2. Methods

2.1. Overview

A synergy is focused to elucidate the different motor functions between elderly and young people. An experiment is conducted to measure body kinematics,

ground reaction force, and muscle electrocardiography data (sEMG) from young and elderly people during standing-up motion. From the obtained sEMG patterns, necessary synergies to achieve the motion are extracted. In addition, two relationships between sEMG patterns and joint torque and between joint torque and body kinematics are developed for individuals to test how muscle synergies contribute body kinematics. Furthermore, extracted synergies are classified into different clusters according to the contribution of synergies to body kinematics. Finally, contribution of synergies and the weaker motor functions of elderly people are clarified.

2.2. Muscle Synergy Analysis

The synergy model in this study regards sEMG patterns as linear combinations of small sets of different synergies [12]. Let d in the model be the number of measured muscles, $t_{\max}$ the maximum time steps of obtained sEMG data, and $\mathbf{m}(t)$ a matrix indicating activation of d muscles during motion at time $t(0 < t \leq t_{\max})$ as shown in Eq. (1). Muscle activation $\mathbf{m}(t)$ is expressed as a vector $\boldsymbol{m}$. Element of $\boldsymbol{m}$ is $(m^1(t), m^2(t), \ldots, m^d(t))^T$ where $m^{(j=1,\ldots,d)}$ represents muscle activation of the j-th muscle.

$$\begin{aligned}\mathbf{m} &= [\boldsymbol{m}(1), \boldsymbol{m}(2), \ldots, \boldsymbol{m}(t_{\max})] \\ &= \begin{pmatrix} m^1(1) & \cdots & m^1(t_{\max}) \\ \vdots & \ddots & \vdots \\ m^d(1) & \cdots & m^d(t_{\max}) \end{pmatrix}. \quad \ldots\ldots \quad (1)\end{aligned}$$

$\mathbf{m}(t)$ is approximated using the linear summation of time-varying synergies $\mathbf{w}_{i=1,2,\ldots,N}(t)$ with non-negative coefficient c_i and onset time delay t_i as shown in Eq. (2). N is the total number of extracted synergies. Synergy is expressed as shown in Eqs. (3)–(4). Elements of $\mathbf{w}_i(t)$ is also expressed as a vector of $(w_i^1(t), w_i^2(t), \ldots, w_i^d(t))^T$ where $w_i^{(j=1,\ldots,d)}$ represents muscle activation of j-th muscle in i-th synergy and T_w is the duration of muscle synergy.

$$\mathbf{m}(t) \cong \sum_{i=1}^{N} c_i \mathbf{w}_i(t - t_i). \quad \ldots\ldots \quad (2)$$

$$\mathbf{w}_i = \begin{pmatrix} w_i^1(1) & \cdots & w_i^1(T_w) \\ \vdots & \ddots & \vdots \\ w_i^d(1) & \cdots & w_i^d(T_w) \end{pmatrix}. \quad \ldots\ldots \quad (3)$$

$$w_j^i(t) = \begin{cases} 0 & (t \leq 0) \\ w_i^j & (0 < t \leq T_w) \\ 0 & (T_w < t). \end{cases} \quad \ldots\ldots \quad (4)$$

Figure 1 shows the schematic design of the synergy model. Three muscle synergies are shown in solid lines, dashed lines, and solid lines with circle markers respectively (**Fig. 1(a)**) and observed d muscle patterns are displayed in gray graphs (**Fig. 1(b)**). Observed muscle patterns during human motion are expressed as a linear summation of 3 synergies with coefficient ($c_{1,2,3}$) and onset time delay ($t_{1,2,3}$) shown as vertical solid black arrows and horizontal dashed black arrows in **Fig. 1(c)**.

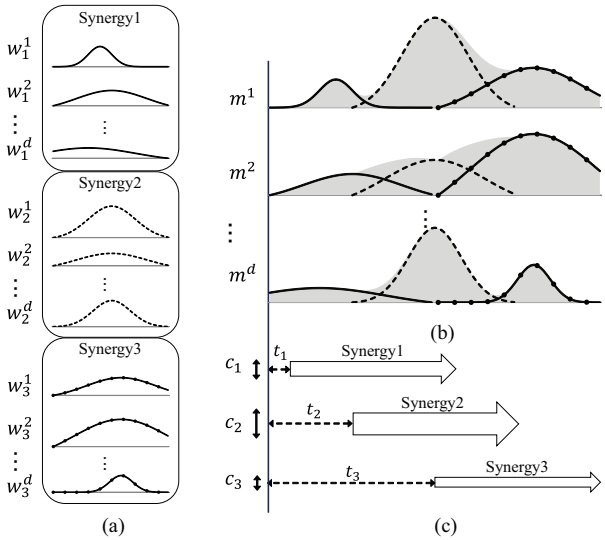

Fig. 1. Synergy model: sEMG patterns are expressed as a linear summation of 3 synergies with non-negative coefficient ($c_{1,2,3}$) and onset time delay ($t_{1,2,3}$). (a) represents 3 sets of muscle synergies. (b) represents d muscle sEMG patterns. (c) represents synergy onset time delay (horizontal dashed arrows) and synergy weighting coefficient (vertical solid arrows) of synergies.

Different strategies of motions are achieved by changing values of c_i and t_i for each synergy. When c_i is changed, the muscle excitation level in synergies is controlled and the time for starting each synergy is adjusted by the value of t_i.

2.2.1. Muscle Synergy Extraction

A non-negative matrix factorization, i.e., a decomposition algorithm, is used to determine synergy patterns and time delays for each synergy [13]. The algorithm uses the multiplicative update rule to optimize elements of synergies $\mathbf{w}_i$, non-negative coefficients c_i, and time delays t_i.

The decomposition algorithm assumes that muscle activation $\mathbf{m}$ is expressed as linear summation of muscle synergies $\mathbf{w}_i$ with weighting coefficient c_i and onset time delay t_i. The decomposition algorithm finds the muscle synergies $\mathbf{w}_i$, weighting coefficient c_i, and onset time delay t_i that minimize squared error (E^2) between observed muscle activation ($\mathbf{m}$) and reconstructed activation from muscle synergies as shown in Eq. (5).

$$E^2 = \operatorname{trace}\left(\mathbf{m} - \sum_{i=1}^{N} \mathbf{w}_i \mathbf{H}_i(c_i, t_i)\right)^{\mathrm{T}} \left(\mathbf{m} - \sum_{i=1}^{N} \mathbf{w}_i \mathbf{H}_i(c_i, t_i)\right) \quad (5)$$

In the equation, $\mathbf{H}(c_i, t_i)$ is the matrix ($T_w \times t_{\max}$) which has the function of scaling muscle synergies with coefficient c_i and shifting with time t_i (Eqs. (6)–(7)).

$$\mathbf{H}(c_i, t_i) = \begin{pmatrix} h_1^1 & \cdots & h_1^{t_{\max}} \\ \vdots & \ddots & \vdots \\ h_{T_w}^1 & \cdots & h_{T_w}^{t_{\max}} \end{pmatrix}. \quad \ldots\ldots \quad (6)$$

$$h_k^l = \begin{cases} 0 & (l \leq t_i) \\ c_i & (t_i \leq l < t_i + T_w, l = k) \\ 0 & (t_i + T_w < l) \end{cases}. \quad \ldots\ldots (7)$$

The following steps are conducted in order to decide muscle synergy pattern, weighting coefficient, and onset time delay:

Step 1: Initial patterns of muscle synergy are determined randomly in this study.

Step 2: In order to minimize E^2, it is necessary to find the onset time delay t_i^{opt} for muscle synergy $\mathbf{w}_i$ that maximize the following function (Eq. (8)):

$$\varphi = \sum_{t=0}^{t_{\max}} \boldsymbol{m}(t)^{\mathrm{T}} \mathbf{w}_i (t - t_i). \quad \ldots\ldots (8)$$

All possible values for t_i are tested to determine t_i^{opt}.

Step 3: Weighting coefficient c_i is updated with calculated onset time delay t_i^{opt} by the following equation (Eq. (9)):

$$c_i^{\text{new}} = c_i \left(\frac{\text{trace}(\mathbf{m}^{\mathrm{T}} \tilde{\mathbf{m}})}{\text{trace}(\tilde{\mathbf{m}}^{\mathrm{T}} \tilde{\mathbf{m}})} \right), \quad \ldots\ldots (9)$$

$$\tilde{\mathbf{m}} = \sum_{i=1}^{N} \mathbf{w}_i \mathbf{H} \left(c_i, t_i^{\text{opt}} \right), \quad \ldots\ldots (10)$$

where $\tilde{\mathbf{m}}$ is the muscle activity pattern generated from muscle synergies by Eq. (10).

Step 4: Component of muscle synergies w_i^j is updated from Eq. (11):

$$w_i'^j(t) = w_i^j(t) \left(\frac{m^j(t)}{\tilde{m}^j(t)} \right). \quad \ldots\ldots (11)$$

Repeat Step 2 to Step 4 until E^2 converges. This decomposition algorithm is repeated 10 times in order to avoid finding only local minima. The best muscle synergy $\mathbf{w}_i$ and onset time delay t_i to minimize E^2 are selected as a solution.

Cross-validation method is employed in order to evaluate model accuracy. Synergy patterns are first calculated from random selected trials of observed data, and model accuracy is tested from applying these synergy models to the rest of observed data. Coefficient of determination (R^2) is used for model accuracy. Cross-validation is repeated 20 times for different random data divisions.

The number of muscle synergies to be extracted is determined from the cross-validation method because it may be different among individuals or it depends on their strategies of the standing-up motion. To ascertain the number of synergies, the accuracy of the model is calculated for different numbers of synergies to test how many synergies are superior for representing the standing-up motion. In order to decide the number of synergies, one factor analysis of variance (ANOVA) is performed to assess the effect of the number of synergies on the accuracy of the model. If there is a statistical significance, a post hoc test (Tukey-Kramer) is performed for each neighboring numbers of synergies. Significance level (p) is set to 0.05 in this analysis.

2.2.2. Joint Torque and Body Kinematics Estimate

The model with 4 links and 3 joints (shown in **Fig. 2**) is used to represent the human body. Planer movement of standing-up motion is focused on because flexion and extension of joint excursion mainly occur in the sagittal plane of body. From our experiment, 3 joint angles, $\theta_{i\{i=\text{ankle,knee,hip}\}}$, are obtained. Three joint torque, $\tau_{i(i=\text{ankle,knee,hip})}$, are calculated using inverse dynamics calculations as shown in Eq. (12),

$$\mathbf{M}(\theta)\ddot{\theta} + \mathbf{h}(\theta, \dot{\theta}) + \mathbf{g}(\theta) + \mathbf{R} = \tau. \quad \ldots\ldots (12)$$

$\mathbf{M}(\theta)$ indicates an inertia term, $\mathbf{h}(\theta, \dot{\theta})$ indicates an imaginary force term, $\mathbf{g}(\theta)$ indicates a gravity term, and $\mathbf{R}$ indicates a ground reaction term. Link length is measured in our experiment, and positions of center of mass and weight of each links are determined by the statistical data of individual body information [14].

To understand how human body motion is generated from synergies, the relationships between sEMG and body kinematics are developed for individual participants. Two of 3-layer neural networks are used to create mapping between sEMG patterns and joint torque, and between joint torque and body kinematics (**Fig. 2**) [15]. In our neural networks, muscular tension generates joint torque and torque activates joints to achieve motion, so firstly sEMG patterns are used to estimate joint torque, $\tau_{i=\text{ankle,knee,hip}}$ (NN1). In addition, joint torque and their body positions $\theta_{i=\text{ankle,knee,hip}}(t)$ and $\dot{\theta}_{i=\text{ankle,knee,hip}}(t)$ at time t are used to estimate body kinematics in the subsequent period $\theta_{i=\text{ankle,knee,hip}}(t + \mathrm{d}t)$ and $\dot{\theta}_{i=\text{ankle,knee,hip}}(t + \mathrm{d}t)$ (NN2). The schematic design of motion estimation is shown in **Fig. 2**. Input variables b_1 and b_2 indicate biased threshold that are added to neural networks, NN1 and NN2. In order to train these neural networks and update weight between nodes and biased threshold b_1 and b_2, all data observed in our experiment – sEMG, joint torque, and joint angles – are used. A cross-validation is used to calculate model accuracy with coefficients of determination R^2. A detailed configuration of the neural network is shown in **Table 1**.

2.2.3. Synergy Classification

To compare synergies among individuals, all extracted muscle synergies are classified into several groups based on synergy contribution toward body kinematics of the standing-up. To explain individual function of synergy, changed muscle patterns are generated by weakening particular patterns of one synergy. Different body kinematics are generated by putting these changed muscle patterns through learned neural networks. This difference is at-

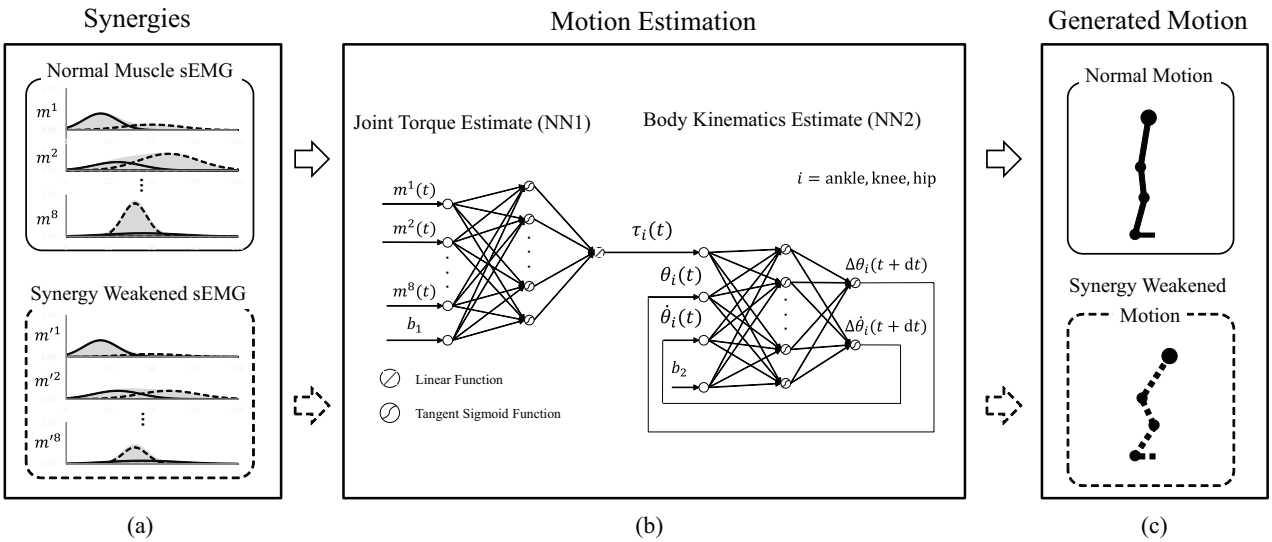

Fig. 2. Estimation of joint torque and body kinematics and synergy effect computation: above figure shows methodology of joint torque and body kinematics estimation and calculation of contribution of synergies toward body kinematics. (a) shows a synergy model used in this study. In this example, eight muscle activations consist of two synergies (solid and dashed lines). The top patterns (normal muscle sEMG) indicate observed sEMG in our experiment whereas the bottom patterns (synergy weakened sEMG) are used to analyze the effect of particularly weakened synergy. (b) shows the neural networks which estimates body kinematics from sEMG patterns. (c) shows the link model used in our study. Solid arrows indicate the normal motion generation, whereas the dashed arrows indicate the changed motion caused by the synergy-weakened muscle patterns. Differences between normal motion and synergy weakened motion are compared to elucidate the effects of synergies.

Table 1. Neural network configuration.

	NN1	NN2
Number of Input Nodes	8	9
Number of Output Nodes	3	6
Number of Hidden Nodes	15	5
Transfer Function of Hidden Nodes	Tangent Sigmoid	
Transfer Function of Output Nodes	Linear	Tangent Sigmoid
Learning Rule	Levenberg-Marquardt	
Number of Training Iterations	20	10

tributable to the specific weakened synergy, which shows the effect of synergies.

To prepare these changed muscle patterns, it is necessary to change the coefficient of the extracted synergy. Eq. (13) shows how synergy-weakened muscle patterns are generated. In the equation, $m'^j(t)$ represents synergy-weakened muscle activation of the j-th muscle at time t, c'_i is the changed coefficient of i-th weakened synergy, c_i is the actually calculated coefficient, N represents the total number of extracted synergies, and t_i is the time delay for i-th synergy. c'_i is set to 75% of original coefficient c_i.

$$m'^j(t) = \frac{\sum_i^N c'_i w_i^j(t-t_i)}{\sum_i^N c_i w_i^j(t-t_i)} m^j(t). \quad \ldots\ldots (13)$$

Figure 2 shows normal muscle patterns and synergy-weakened muscle patterns. This example includes muscle activation of 8 muscles approximated by 2 synergies (shown in solid lines and dashed lines). Synergy-weakened muscle patterns, described at bottom of **Fig. 2(a)**, are generated by weakening one synergy shown by dashed lines.

We calculate the percentage of changes using Eq. (14) to evaluate synergy contribution. The degree of absolute change between normal body kinematics and changed kinematics is calculated for the whole duration of the motion. In the equation, $\theta_{i=\text{ankle,knee,hip}}(t)$ shows the joint angles of the ankle, knee, and hip at certain time t which are generated from normal muscle activation. $\theta'_i(t)$ is calculated from weakened synergy muscle patterns. Changed body kinematics are calculated from all trials of all participant.

$$sc_{i=\text{ankle,knee,hip}}(t) = \frac{|\theta_i(t) - \theta'_i(t)|}{\theta_i(t)}. \quad \ldots\ldots (14)$$

In this study, the synergy contribution to body kinematics is calculated as the average of $sc_{i=\text{ankle,knee,hip}}(t)$ between four phases of standing-up motion; the synergy contribution vector in Eq. (15) is used to represent synergy contribution in four phases. In the equation, i signifies the number of participants, and j denotes the ordinal number of synergies extracted from participants. Hence, $sc^{k=\text{I,II,III,IV}}_{\theta_{l=\text{ankle,knee,hip}}}$ shows the average of synergy contribution on a specific joint angle l during a particular phase k.

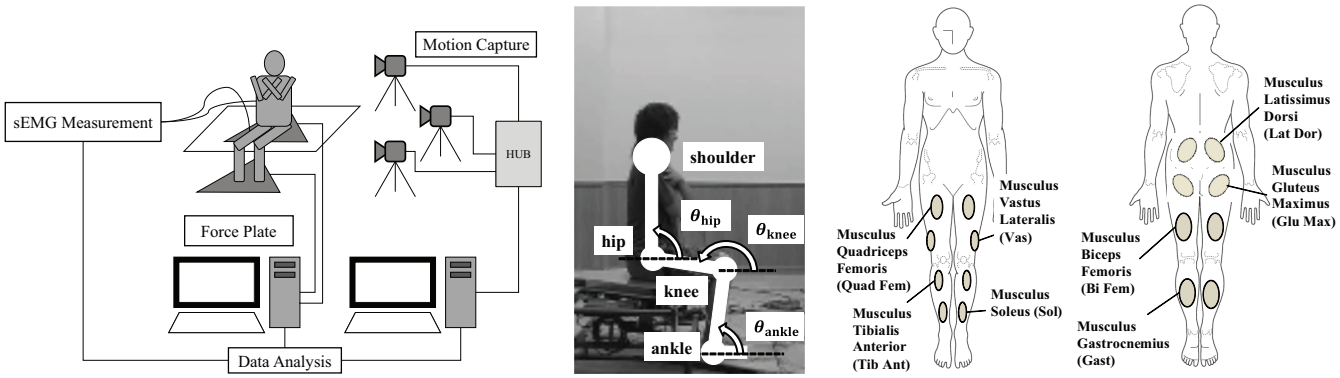

(a) Experimental setup (b) Link model (c) Measured sEMG

Fig. 3. Experiment design: (a) Schematic design of experimental setup. (b) Motion capture sensor sites. Sensors were attached to the shoulder, hip, knee, and ankle. (c) Muscle activation was obtained from 16 muscles described above.

$$\mathbf{sc}_i^j = [\ sc^{\mathrm{I}}_{\theta_{\mathrm{ankle}}} sc^{\mathrm{II}}_{\theta_{\mathrm{ankle}}} sc^{\mathrm{III}}_{\theta_{\mathrm{ankle}}} sc^{\mathrm{IV}}_{\theta_{\mathrm{ankle}}} \\ sc^{\mathrm{I}}_{\theta_{\mathrm{knee}}} sc^{\mathrm{II}}_{\theta_{\mathrm{knee}}} sc^{\mathrm{III}}_{\theta_{\mathrm{knee}}} sc^{\mathrm{IV}}_{\theta_{\mathrm{knee}}} \\ sc^{\mathrm{I}}_{\theta_{\mathrm{hip}}} sc^{\mathrm{II}}_{\theta_{\mathrm{hip}}} sc^{\mathrm{III}}_{\theta_{\mathrm{hip}}} sc^{\mathrm{IV}}_{\theta_{\mathrm{hip}}}]. \quad (15)$$

2.2.4. Cluster Analysis

In this paper, cluster analysis is used to classify extracted synergies based on contribution on body kinematics. Synergies' effects on body kinematics are different among synergies because body kinematics ($\theta(t+\mathrm{d}t)$, $\dot{\theta}(t+\mathrm{d}t)$) is decided from both muscle activation generated by synergies and previous body kinematics ($\theta(t)$, $\dot{\theta}(t)$). Each synergy therefore has different effects on body kinematics although their patterns or time delays are similar.

K-means cluster analysis is used to classify synergies based on their contribution matrix. In the procedure, similar synergies are distributed in the same cluster. To calculate their similarity, the cosine of 2 synergy contribution vectors, $\mathbf{sc}_i^j$, is used. In order to decide the number of clusters in K-means cluster analysis, we test different numbers of clusters from 2 to 5. The average of cosine of vectors between data and a mid point of a cluster is used to evaluate the classification performance based on the number. If this average is small, there are many data far from the mid point of clusters, so more clusters are needed. This K-means cluster analysis is applied for 100 times with random initial data divisions. One factor repeated measures analysis of variance (ANOVA) is performed to assess effect of the number of clusters, with post hoc two sided Tukey's simultaneous tests when appropriate. The significance level is set to $p = 0.05$.

2.3. Experiment

2.3.1. Experimental Setup

Figure 3(a) shows our experimental system to measure participant body kinematics, ground reaction force, and sEMG data during standing-up motion. MAC3D System (HMK-200RT; Motion Analysis) with 8 cameras was used to measure body kinematics. Before recording start, we performed calibration to confirm the accuracy of the system. The body kinematics data were obtained at 64 Hz. Four body parts were recorded during experiment to construct a link model of participant: shoulder, hip, knee, and ankle. **Fig. 3(b)** shows marker positions attached to participants to express the link model. Joint angles were calculated as angles between each link and a horizontal direction.

In this study, 2 force plates were used to measure vertical reaction force from the hips and feet at 4 Hz. We originally built a force plate with a six-axes force sensor system (IFS-90M40A; Nitta Corp.). These forces were used to calculate ankle, knee, and hip joint torque of individual participant from inverse dynamics calculation.

Personal-EMG (Oisaka Electronics Device Ltd.) was used to record sEMG from 8 kinds of muscles (**Fig. 3(c)**). These muscles were chosen as flexor and extensor of ankle, knee, and hip joints. Data were obtained at 1600 Hz, and they were filtered with a 10 Hz hi-pass filter and 50–60 Hz hum noise filter with a filter box of the system.

2.3.2. Data Processing

Measured 3-dimensional body kinematics data were orthogonally projected onto a sagittal plane of participants in order to construct a 2-dimensional link model. Joint angles, joint torque, and center of mass were calculated based on inverse dynamics calculation, body kinematics and ground reaction force data.

All sEMG data were centered and rectified. Both left and right muscles were averaged to represent one muscle. sEMG data were filtered by the smoothing filter calculated using Eq. (16). In the equation, i is the number of observed muscle and t is the discrete time step of the data. sEMG data were averaged for 0.2 s (320 points of data). Additionally, data of joint torque and angular velocity were averaged as well.

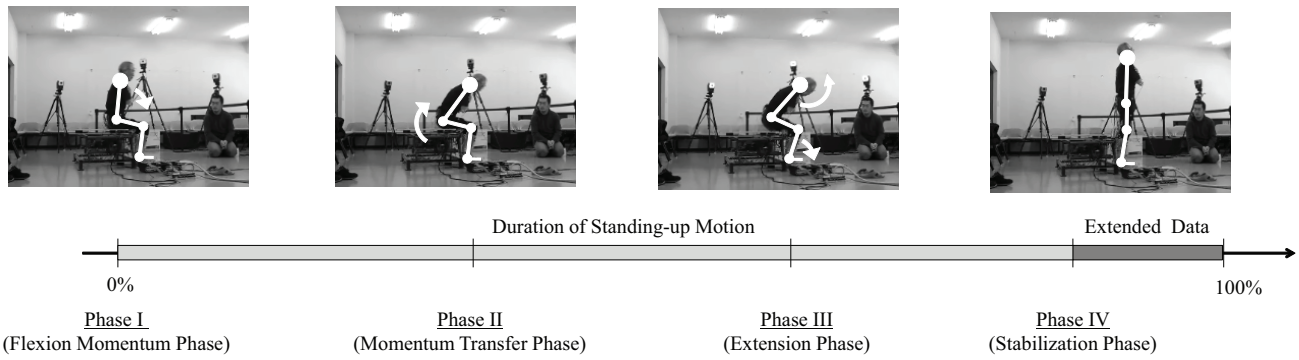

Fig. 4. Four phases division: the four pictures portray postures of participants during phases. Data were normalized based on the start point of each phase.

$$m^i_{\text{filtered}}(t) = \frac{\sum_{t'=0}^{319} m^i(t-t')}{320} \quad \ldots\ldots\ldots (16)$$

2.3.3. Data Normalization

Because the duration of the standing-up motion differ among participants, it is necessary to normalize the standing-up motion to compare different trials of participants. It is also important to understand the effect of synergies from the viewpoint of human body kinematics because it has been reported that muscle synergy corresponds to kinematic events in human motion [10]. Consequently, 4 characteristic points of human standing-up motion are chosen and each phase between points is addressed. These 4 phases are decided from the earlier study [16], and they have been widely used to analyze the human standing-up motion [17]. The start point of each phase is defined as follows.

- Phase I (Flexion Momentum Phase)
  It begins with first shoulder movement in the horizontal direction.
- Phase II (Momentum Transfer Phase)
  It begins with the first hip movement in the vertical direction.
- Phase III (Extension Phase)
  It begins when the ankle angle achieves the minimum flexion.
- Phase IV (Stabilization Phase)
  It begins when the vertical shoulder position achieves the maximum height.

The end of Phase IV is determined by extending the time series past the beginning of Phase IV by an additional 20% of the duration of Phases I–III. In addition to the phase division, all data of the motion are normalized to 100% based on total movement time. For normalization, the beginning point of the motion is determined at the start of phase I. The end of the motion is chosen at the end of Phase IV. **Fig. 4** shows a description of each phase and how we normalized data.

2.3.4. Participants

Ten persons with no noted impairments participated in our experiment. The number of participants in this study was sufficient for analysis compared to the number of participants of previous studies (8, 9 and 10 people) that conducted the similar experiments to measure body kinematics, reaction force, and muscle activation [18–20]. These participants (P1–P10) were divided into 2 groups: a younger group ($N = 3$, P1–P3; mean age = 24.0 years, standard deviation (STD) = 3.5 years) and an elderly group ($N = 7$, P4–P10; mean age= 67.1 years, STD = 7.3 years). During experiments, participants were told to stand up in a way they found comfortable. The number of trials they performed during our experiments differed among participants ranging between 12 to 20 trials. Before experiments were started, all participants were confirmed to be able to stand up and maintain a standing posture without any assistance. We have also explained experiments in detail and obtained written consent from all participants.

3. Results

3.1. Synergy Extraction

The number of synergies to be extracted from observed sEMG patterns was clarified using the cross-validation method. The measured trials of standing-up motion were randomly divided into training and test data set for cross validation as follows: 15 trials were obtained for P1 and were divided into 12 training data and 3 test data, 12 trials were obtained for P2 and were divided into 10 training data and 2 test data, 16 trials were obtained for P3 and P8 and were divided into 12 training data and 4 test data, 18 trials were obtained for P4, P5, and P7, and were divided into 15 training data and 3 test data, and 20 trials were obtained for P6, P9, and P10 and were divided into 16 training data and 4 test data.

Changes in coefficients of determination R^2 based on the number of synergies are shown in **Fig. 5**. Error bars in the graph show standard deviation of coefficients of determination. ANOVA showed a statistical significance of

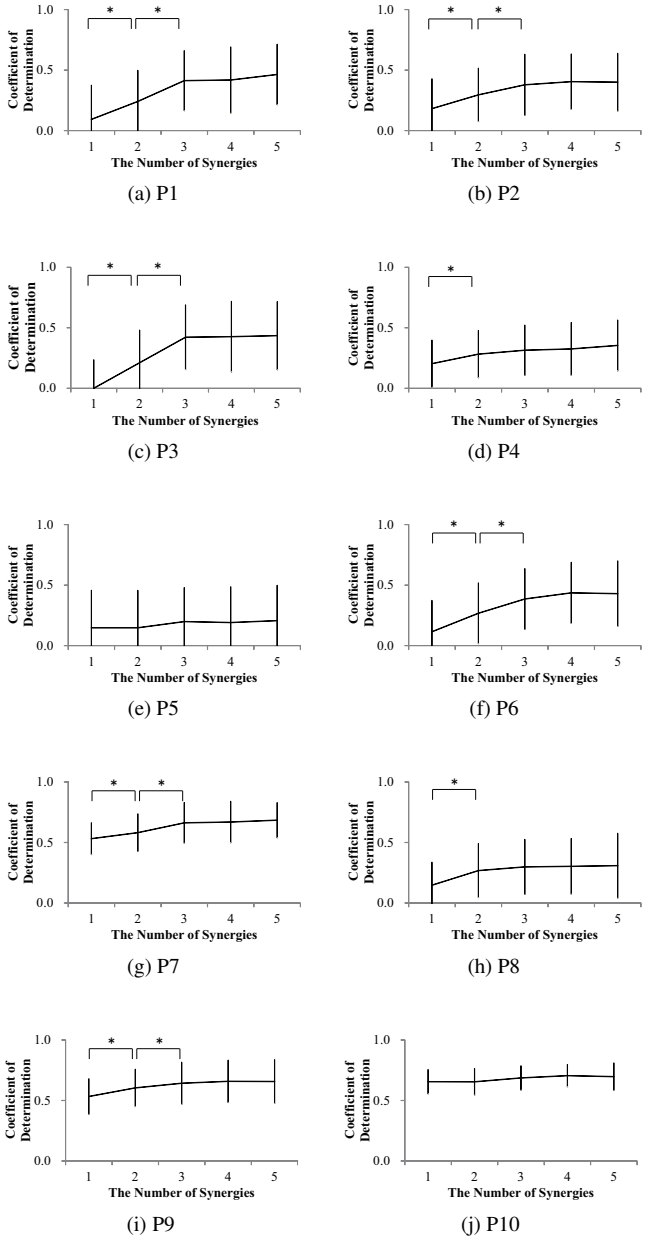

Fig. 5. Coefficient of determination for participants: calculated averaged coefficients of determination based on the change in the number of synergies are shown for all participants. Error bars show standard deviation.

P1, P2, P3, P4, P6, P7, P8, and P9. The post hoc test was applied to neighboring numbers of synergies for data of showing statistical significance in ANOVA. Statistical significance was found between 1 and 2 and between 2 and 3 for P1, P2, P3, P6, P7, and P9. There was a statistical significance between 1 and 2 for P4 and P8. From this statistical analysis, the number of synergies was determined from how additional synergies contributed to improving performance, so the number of synergies was set to 1 for P5 and P10, to 2 for P4 and P8, and to 3 for P1, P2, P3, P6, P7, and P9.

Table 2. Number of synergies and time delay for participants.

	Number of Synergies	Average Time Delay		
P1	3	0	9	34
P2	3	0	10	43
P3	3	0	21	35
P4	2	29	53	–
P5	1	49	–	–
P6	3	−1	12	36
P7	3	3	30	44
P8	2	33	73	–
P9	3	28	41	48
P10	1	46	–	–

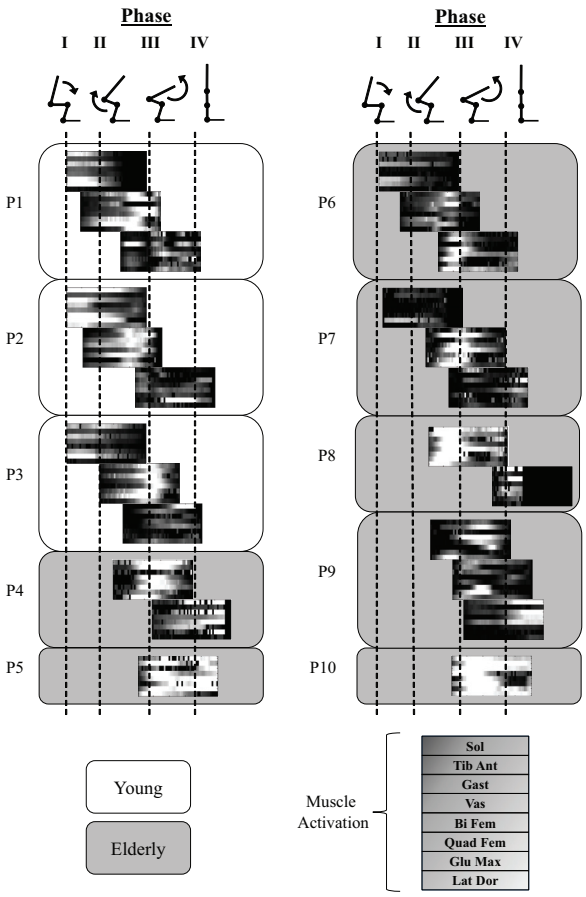

Fig. 6. Extracted synergy patterns: squares shown above represent extracted synergies from young participants (white) and elderly participants (gray). Each row indicates different muscles and the X-axis shows time steps. The brighter the color is, the more activated each muscle is. Offsets of each synergy indicate their time delays. Vertical dashed lines show start points of 4 phases.

Table 2 shows the number of extracted synergies and their time delays. Results of extracted synergy patterns are shown in **Fig. 6** with time delays. Each square in the figure is an extracted synergy represented in a gray scale.

Table 3. Mean distance between data and the mid point of clusters.

	Coefficient of Determination
τ_{ankle}	0.75 ± 0.29
τ_{knee}	0.91 ± 0.16
τ_{hip}	0.81 ± 0.16
θ_{ankle}	0.77 ± 0.21
θ_{knee}	0.95 ± 0.09
θ_{hip}	0.72 ± 0.16
$\dot{\theta}_{\text{ankle}}$	0.74 ± 0.16
$\dot{\theta}_{\text{knee}}$	0.88 ± 0.09
$\dot{\theta}_{\text{hip}}$	0.76 ± 0.15

The brighter the color is, the more activated each muscle is. The Y-axis depicts 8 measured muscles of different types. Onsets for each square indicate time delays of the represented synergy and vertical dashed lines show start points of 4 phases.

3.2. Results of Cluster Synergies

The musculoskeletal model was expressed as 2 neural network models to express relationships between sEMG and joint torque and between joint torque and body kinematics. Cross validation was used to evaluate the accuracy of neural networks. The same number of training and test data set was used for participants as in validation of muscle synergy extraction. **Table 3** shows the average and standard deviation of coefficient of determination, R^2 for estimating joint torque, joint angle, and angular velocity.

Synergy-weakened muscle patterns were put into trained neural networks, and synergy contribution vectors (**sc**) were calculated for all 24 synergies from 10 participants. Body kinematics ($\theta(t+\mathrm{d}t)$ and $\dot{\theta}(t+\mathrm{d}t)$) were recurrently determined from the past body posture ($\theta(t)$ and $\dot{\theta}(t)$), so although duration of some muscle synergy was only seen in specific phases, they affected body kinematics in posterior phases. K-means cluster analysis was applied to synergy contribution vectors. In this study, dt was normalized time step.

Statistical analysis found statistical significance for all neighboring number of clusters to be as follows: between numbers of 2 and 3, 3 and 4, and 4 and 5. The average distance between synergies and mid point of each cluster is shown in **Table 4**. The number of clusters was set to 4. If the number of clusters was more than 4, then the new cluster only included a single data. Consequently, it seemed to improve the performance, but the additional cluster caused segmentalization.

Figure 7 demonstrates the average synergy contribution of 4 clusters toward joint angles among 4 phases. The X-axis shows four phases and the Y-axis shows the mean percentage of contribution to each joint angle. Error bars indicate standard deviation of synergy contribution. White bars show contribution toward an ankle angle.

Table 4. Mean distance between data and the mid point of clusters.

Number of Clusters	Average Distance	STD
2	0.395	0.023
3	0.522	0.057
4	0.532	0.039
5	0.553	0.020

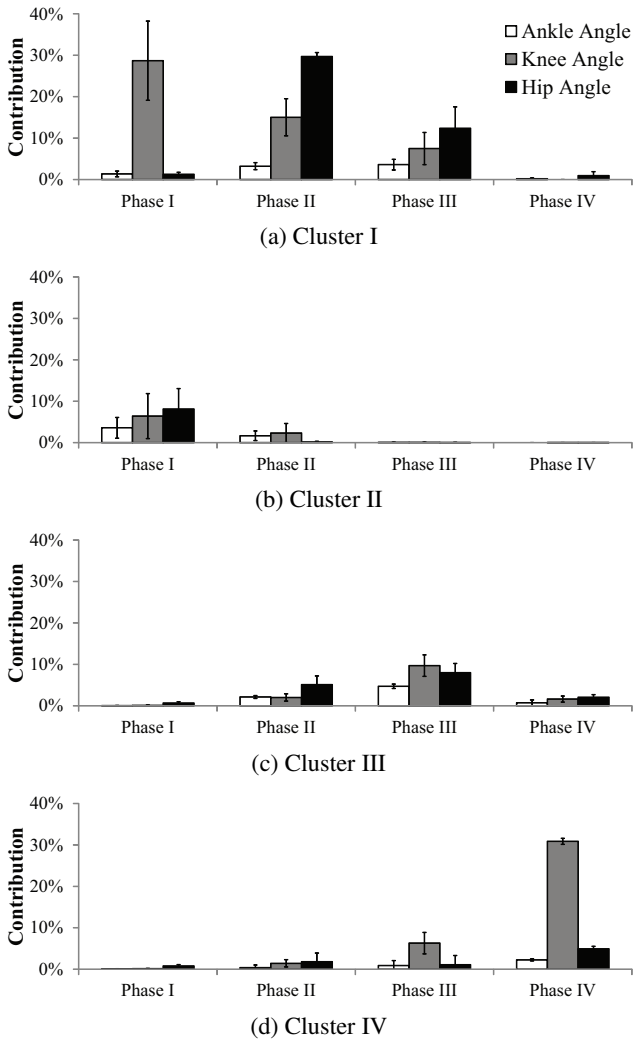

(a) Cluster I

(b) Cluster II

(c) Cluster III

(d) Cluster IV

Fig. 7. Average contribution of synergies in clusters: bar graphs show average contributions of synergies included in 4 clusters. Error bars show standard deviation. Contributions to each joint angle was averaged during each phase. The Y-axis shows their contribution based on original angles.

Gray bars show contribution to a knee angle, and the black bars show contribution to a hip angle. Synergies involved in each cluster was as follows: the i-th synergy of the j-th participant is expressed as Pj-i, e.g., P1-2 indicates the second synergy of P1.

- Cluster I: P1-1, P1-2, P2-2, P3-1
- Cluster II: P6-1, P6-2, P7-3

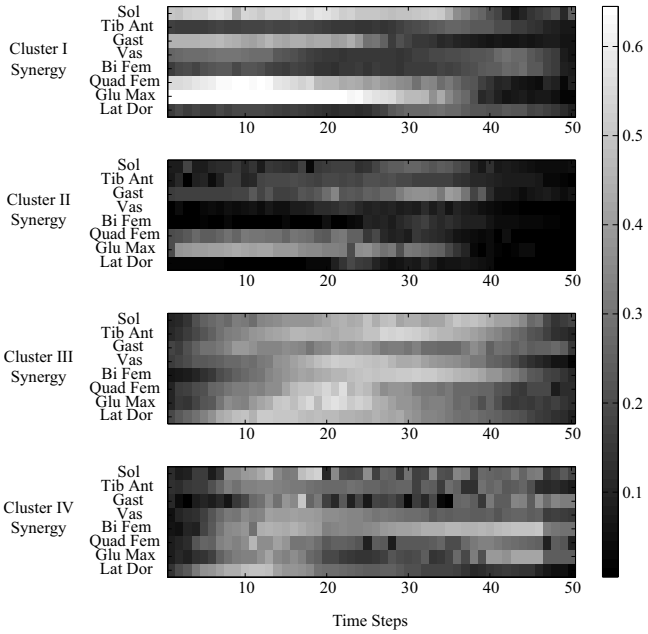

Fig. 8. Average synergy patterns in clusters: average synergy patterns are shown in each cluster. The brighter the color is, the more activated each muscle is. The Y-axis shows different muscles and the X-axis shows time steps during synergies.

- Cluster III: P1-3, P2-1, P2-3, P3-2, P3-3, P4-1, P7-2, P8-1, P9-1, P9-2, P10-1
- Cluster IV: P4-2, P6-3, P5-1, P7-1, P8-2, P9-3

Figure 8 shows averaged synergies in the 4 clusters. The brighter the color is, the more activated muscle is. Y-axis shows 8 different muscles.

4. Discussion

4.1. Synergy Extraction

Muscle synergies were extracted from observed sEMG patterns during standing-up motion. After cross validation, synergy patterns were decided based on all observed sEMG data. The decomposition algorithm was repeated 20 times for each subject, and a set of synergy was chosen that showed the highest coefficients of determination. The number of synergies to be extracted differed between participants. Three synergies were extracted from all young participants, whereas the number of synergies were 1–3 for the elderly. Among individuals, strategies of standing-up motion might differ, which would account for difference in the number of synergies. Different standing-up strategies indicate that muscles were activated differently depending on the strategy. Specifically, low muscle activation was found in prior phases for those who used only 1 synergy (P5 and P10) whereas there was comparatively higher muscle activation observed in the earlier phase for young participants who had 3 synergies.

4.2. Body Kinematics Estimation

To estimate joint torque and body kinematics, 2 neural networks were used in this study. Estimation results for joint torque, angle, and angular velocity showed a high value, which implied that it was able to estimate body kinematics from sEMG patterns. Coefficients of determination, R^2, differed in outputs of the neural networks. Specifically, result for the knee and hip showed better estimation results than result for the ankle – a difference was mainly attributable to sEMG input data. Among 8 inputs of NN1, muscles of 4 kinds were attached to a knee and 5 attached to a hip to exert a force on it. This was more than the number of muscles related to a ankle joint (3 muscles), so inputs of NN1 contained more information about a knee than an ankle joint. Even so, musculoskeletal systems were developed for all subjects. Neural networks were trained with all observed data after cross validation and trained networks were used for calculating the contributions of synergies.

4.3. Contributions of Synergies

From cluster analysis, synergies in 4 clusters (Clusters I–IV) were determined based on their effects on joint angles in each phase. Since body kinematics was affected by previous body postures in neural networks, extracted synergies were classified based on their effects on body kinematics although the time delay or patterns of synergies in each cluster differed. Average muscle activation of synergies in each cluster is discussed below (Clusters I–IV Synergy).

4.3.1. Cluster I Synergy

All synergies included in the Cluster I were extracted from the young group. Based on time delays, these synergies started from the beginning of the standing-up motion (mean time delay = 2.25, STD = 4.50). In terms of contributions to each joint, synergies in Cluster I mainly affected a knee joint in both Phases I and II and a hip joint in Phase II. Specifically, in Phase II, which was the start point of momentum transfer, a motion of lifting-up a hip was distracted by weakened synergies belonging to the Cluster I. **Fig. 8** supports this perspective. The activated muscles were the musculus soleus and musculus gastrocnemius, which were related to the ankle, and musculus biceps femoris and musculus gluteus maximus, which contributed to the hip. This synergy was thus presumed to work when participants flexed their feet and bent their backs to lift the hip.

4.3.2. Cluster II Synergy

Synergies in Cluster II seemed to work similarly to synergies in Cluster I Synergy. Those synergies were extracted only from the elderly group, involving 2 participants, which implied that not all elderly participants had this type of synergies. All these synergies started at the beginning of the standing-up motion based on time delays (mean time delay 4.67, STD = 6.66). **Fig. 8** shows that the

musculus gastrocnemius, musculus quadriceps femoris, and musculus gluteus maximus were activated in the average synergy. The average activation of these muscles was, however, weaker and its contribution to the hip angle in Phase II was also smaller than that of Cluster I Synergy.

4.3.3. Cluster III Synergy

Cluster III included synergies extracted from most participants (8 participants). Synergy patterns in **Fig. 8** show that all muscles were activated, and those synergies started from the middle of the motion (mean time delay = 32.81, STD = 10.22). This synergy mainly contributed to movement in Phase III, such as extension of whole body. Results of synergy contributions in the Cluster III (**Fig. 7**) show that Cluster III Synergy affected all 3 joint angles in the Phase III in which people moved all 3 joints to lift up their upper body vertically. Without this synergy, people cannot lift up their hip during standing-up motion.

4.3.4. Cluster IV Synergy

Synergies in Cluster IV were extracted from elderly participants only. These synergies started at the latter phase of the standing-up motion (mean time delay = 50.39, STD = 13.64), and they contributed to the knee in Phase III and all 3 angles in Phase IV. The average synergy pattern in **Fig. 8** shows that the musculus soleus, musculus gastrocnemius, musculus biceps femoris, and musculus gluteus maximus were activated in Cluster IV Synergy. These muscles were attached and contribute to all 3 joints. Synergies in Cluster IV presumably functioned in stabilizing posture while compensating for the large center-of-mass movement after the standing-up motion was achieved.

4.4. Different Muscle Synergy Between the Young and the Elderly

Extracted synergies from young and elderly participants were classified into 4 clusters clearly showing differences between the 2 groups. Synergies in Clusters I and II functioned similarly; they flexed the ankle and bent their backs. However, only two elderly people had this type of synergies, although all young participants had a synergy in Cluster I. These results implied that some elderly persons had deficient muscle coordination for flexing the ankle and bending trunk to raise the hips. The reason for this deficient motor function might be due to fear avoidance action. Specifically, during Phase II, elderly persons must transfer the center of mass from the hip to feet, which possibly caused them to fall. For such reasons, not all of the elderly had this type of the synergy (the Clusters I and II Synergy).

Cluster III Synergy was extracted from both young and elderly participants and functioned as an extension of their whole body to complete the action of standing-up motion. This suggests that the elderly also coordinated muscles when they extended the body after transferring the center of mass on their feet.

Cluster IV Synergy, which helped stabilize posture, was seen only in elderly participants. This suggests that it was easier for elderly participants than for the young to lose stability as they completed the action of standing-up. Therefore, additional muscle coordination was necessary to stabilize their posture to avoid falling.

5. Conclusions and Future Works

5.1. Conclusions

Synergies important to the standing-up motion were extracted from both young and elderly groups. The effects of these synergies on body kinematics has been calculated by estimating individual body kinematics estimation. Extracted synergies were then classified into several groups based on its effects. Results have shown that muscle synergies were divisible into 4 groups (the Clusters I–IV Synergy). These synergies in each cluster functioned as follows:

1. Cluster I Synergy

   Cluster I Synergy was extracted only from young people and started at the beginning of movement. It worked as flexing the ankle and raising up their hips to move the center of mass from their hips to the feet.

2. Cluster II Synergy

   Cluster II Synergy was extracted only from two elderly people. It functioned similarly to that of Cluster I Synergy. However, muscle activation involved in this synergy was weaker, so its contribution of moving the center of mass was less than that of Cluster I Synergy.

3. Cluster III Synergy

   Cluster III Synergy was observed in both young and elderly participants. This synergy mainly began at the middle of the standing-up motion and affected extending the upper body.

4. Cluster IV Synergy

   Cluster IV Synergy was obtained only from some elderly participants. This synergy began at the latter phases of the standing-up motion. It stabilized posture after standing-up motion was completed.

Cluster analysis explained the difference between the young and the elderly in terms of synergies. Compared to the young, some elderly persons had weaker synergy (Cluster II Synergy) or had no synergy at all for flexing their ankle and bending to raise their hip from a chair. Results also showed that some of the elderly needed additional synergy to stabilize their posture after the action of standing-up had been completed.

5.2. Future Works

This study has clarified the difference between the young and the elderly people in terms of synergy. Deficient or additional synergies were found from some of the elderly but not in the young. Experiments and synergy analysis were performed only on the healthy elderly people, so it would be an interesting to conduct additional analysis on those with specific disorders, e.g., brain injury. If synergies is related to disorders or injuries, such knowledge could be useful in rehabilitation or assistive device to support and enhance body function.

Another future direction of our study is to implement these findings in new training methods strengthening the weaker synergy and corresponded body movements. Essential muscle synergies to perform the standing-up motion have been extracted in this study. Results reported from previous research suggest that individuals should train their motor functions in the context of motion to coordinate joint and muscle movements [21]. In training motor functions involving bending forward to raise their hip, they should work on exercises involving the same muscle activation as the extracted synergies. Squatting, for example, is one choice in training that trains almost all muscles involved in Cluster III Synergy. It surely strengthens muscles and enhances the ability of extending the joints. However, squatting requires keeping the back straight up, and the exercise is usually conducted in the static position, which differs from the posture used during Phase III. Therefore, it is necessary to train deficient motor control in the same context of the standing-up motion.

Individuals who lose or otherwise lack synergies because of injury or disease must regain or relearn them. Results of one study have implied that for those who want to learn a new synergy, it would be the best to firstly try to use another existing synergy from different tasks [22]. For those who have a similar synergy, they should just train it intensely. If no synergy is appropriate for the standing-up motion, then they must train and reconstruct it again. Assistive robotics should thus specifically examine this lost synergy for support or for training.

Acknowledgements

This research was in part supported by MEXT KAKENHI, Grant-in-Aid for Scientific Research (B) 24300198, and Grant-in-Aid for JSPS Fellows 24·8702. Authors thank Dr. Kaoru Takakusaki of Asahikawa Medical University for giving us the instruction to conduct safe experiment.

References:

[1] K. Andersen-Ranberg, K. Christensen, B. Jeune, A. Skytthe, L. Vasegaard, and J. W. Vaupel, "Declining physical abilities with age: a cross-sectional study of older twins and centenarians in Denmark," Age and Ageing, Vol.28, No.4, pp. 373-377, 1999.

[2] P. G. Huston, "Family care of the elderly and caregiver stress," American Family Physician, Vol.42, No.3, pp. 671-676, 1990.

[3] J. M. Guralnik, E. M. Simonsick, L. Ferrucci, R. J. Glynn, L. F. Berkman, D. G. Blazer, P. A. Scherr, and R. B. Wallace, "A short physical performance battery assessing lower extremity function: association with self-reported disability and prediction of mortality and nursing home admission," J. of Gerontology, Vol.49, No.2, pp. 85-94, 1994.

[4] J. M. Guralnik, L. Ferrucci, E. M. Simonsick, M. E. Salive, and R. B. Wallace, "Lower-extremity function in persons over the Age of 70 years as a predictor of subsequent disability," New England J. of Medicine, Vol.332, pp. 556-561, 1995.

[5] M. A. Fiatarone, E. C. Marks, N. D. Ryan, C. N. Meredith, L. A. Lipsitz, and W. J. Evans, "High-intensity strength training in nonagenarians," The J. of the American Medical Association, Vol.263, pp. 3029-3034, 1990.

[6] D. G. Sale and J. D. MacDougall, "Specificity in strength training: a review for the coach and athlete," Canadian J. of Applied Sports Science, Vol.6, pp. 87-92, 1981.

[7] D. M. Buchnder, E. B. Larson, E. H. Wagner, T. D. Koepsell, and B. J. De Lateur, "Evidence for a non-linear relationship between leg strength and gait speed," Age and Ageing, Vol.25, pp. 386-391, 1996.

[8] S. E. Ross and K. M. Guskiewicz, "Effect of coordination training with and without stochastic resonance stimulation on dynamic postural stability of subjects with functional ankle instability and subjects with stable ankles," Clinical J. of Sport Medicine, Vol.16, No.4, pp. 323-328, 2006.

[9] N. Bernstein, "The co-ordination and regulation of movement," Pergamon, Oxford, 1967.

[10] Y. P. Ivanenko, R. E. Poppele, and F. Lacquaniti, "Five basic muscle activation patterns account for muscle activity during human locomotion," The J. of Physiology, Vol.556, pp. 267-282, 2004.

[11] R. R. Neptune, D. J. Clark, and S. A. Kautz, "Modular control of human walking: a simulation study," J. of Biomechanics, Vol.42, pp. 1282-1287, 2009.

[12] A. d'Avella, P. Saltiel, and E. Bizzi, "Combinations of muscle synergies in the construction of a natural motor behavior," Nature Neuroscience, Vol.6, pp. 300-308, 2003.

[13] A. d'Avella, "Decomposition of EMG patterns as combinations of time-varying muscle synergies," First Int. IEEE EMBS Conf. on Neural Engineering 2003, Conf. Proc., pp. 55-58, 2003.

[14] E. C. lauser, J. T. McConville, and J. W. Young, "Weight, volume and center of mass of segments of the human body," Wright-Patterson Air Force Base, Ohio, AMRL Technical Report, pp. 69-70, 1969.

[15] Y. Koike and M. Kawato, "Estimation of dynamic joint torques and trajectory formation from surface electromyography signals using a neural network model," Biological Cybernetics, Vol.73, pp. 291-300, 1995.

[16] M. Schenkman, R. A. Berger, O. R. Patrick, R. W. Mann, and W. A. Hodge, "Whole-body movements during rising to standing from sitting," Physical Therapy, Vol.70, pp. 638-651, 1990.

[17] W. G. M. Janssen, H. B. J. Bussmann, and H. J. Stam, "Determinants of sit-to-stand movement: a review," Physical Therapy, Vol.82, pp. 866-879, 2002.

[18] L. D. W. Vander, D. Brunt, and M. U. McGulloch, "Variant and invariant characteristics of the sit-to-stand task in healthy elderly adults," Archives of Physical Medicine and Rehabilitation, Vol.75, pp. 653-660, 1994.

[19] U. P. Arborelius, P. Wretenberg, and F. Lindberg, "The effects of armrests and high seat heights on lower-limb joint load and muscular activity during sitting and rising," Ergonomics, Vol.35, pp. 1377-1391, 1992.

[20] S. Kawagoe, N. Tajima, and E. Ghosa, "Biomechanical analysis of effects of foot placement with varying chair height on the motion of standing-up," J. of Orthopaedic Science, Vol.5, pp. 124-133, 2000.

[21] D. A. Jones, O. M. Rutherford, and D. F. Parker, "Physiological changes in skeletal muscle as a result of strength training," Quarterly J. of Experiment Physiology, Vol.74, pp. 233-256, 1989.

[22] G. C. Richard, "Changes in muscle coordination with training," J. of Applied Physiology, Vol.101, pp. 1506-1513, 2006.

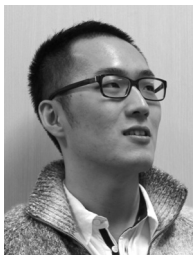

Name:
Qi An

Affiliation:
Department of Precision Engineering, Graduate School of Engineering, The University of Tokyo

Address:
7-3-1 Hongo, Bunkyou-ku, Tokyo 113-8656, Japan

Brief Biographical History:
2009.3 Bachelor of Engineering from The University of Tokyo
2011.9 Master of Engineering from The University of Tokyo
2011.10- Doctoral Course, Department of Precision Engineering, The University of Tokyo
2012.4- Research Fellowship for Young Scientist (DC1), Japan Society for the Promotion of Science

Main Works:
• C. E. Stepp, Q. An, and Y. Matsuoka, "Repeated Training with Augmentative Vibrotactile Feedback Increases Object Manipulation Performance," PLoS ONE, Vol.7, e32743, 2012.

Membership in Academic Societies:
• The Institute of Electrical and Electronics Engineers (IEEE)
• The Robotics Society of Japan (RSJ)
• The Japan Society for Precision Engineering (JSPE)

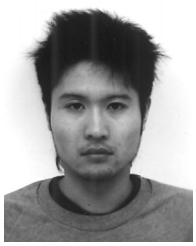

Name:
Yusuke Ikemoto

Affiliation:
Graduate School of Science and Engineering for Research, University of Toyama

Address:
3190 Gofuku, Toyama 930-8555, Japan

Brief Biographical History:
2006- Post-Doctoral Fellow, RACE (Research into Artifacts, Center for Engineering), The University of Tokyo
2009- Post-Doctoral Fellow, Department of Precision Engineering, Graduate School of Engineering, The University of Tokyo
2010- Assistant Professor, Graduate School of Science and Engineering for Research, University of Toyama

Main Works:
• Y. Ikemoto, Y. Ishikawa, T. Miura, and H. Asama, "A mathematical model for caste differentiation in termite colonies (Isoptera) by hormonal and pheromonal regulations," Sociobiology, Vol.54, pp. 841-859, 2009.
• Y. Ikemoto, Y. Hasegawa, T. Fukuda, and K. Matsuda, "Gradual Spatial Pattern Formation of Homogeneous Robot Group," the Int. J. of Information Sciences, Vol.171, No.4, pp. 431-445, 2005.

Membership in Academic Societies:
• The Institute of Electrical and Electronics Engineers (IEEE)
• The Japan Society of Mechanical Engineers (JSME)
• The Society of Instrument and Control Engineers (SICE)

Name:
Hajime Asama

Affiliation:
Department of Precision Engineering, Graduate School of Engineering, The University of Tokyo

Address:
7-3-1 Hongo, Bunkyou-ku, Tokyo 113-8656, Japan

Brief Biographical History:
1986- Research Associate, RIKEN (The Institute of Physical and Chemical Research)
1998- Professor, RACE (Research into Artifacts, Center for Engineering), The University of Tokyo
2002- Professor, Department of Precision Engineering, Graduate School of Engineering, The University of Tokyo

Main Works:
• Y. Ikemoto, T. Miura, and H. Asama, "Adaptive Division-of-Labor Control Algorithm for Multi-robot Systems," J. of Robotics and Mechatronics, Vol.22, No.4, pp. 514-525, 2010.

Membership in Academic Societies:
• The Institute of Electrical and Electronics Engineers (IEEE)
• The Robotics Society of Japan (RSJ)
• The Japan Society of Mechanical Engineers (JSME)
• The Society of Instrument and Control Engineers (SICE)